Ruderman-Kittel theory of oscillatory interlayer exchange coupling

P. Bruno and C. Chappert*
Institut d'Electronique Fondamentale, Bâtiment 220, Université Paris-Sud, F-91405 Orsay CEDEX, France
(Received 13 December 1991)

We present a Ruderman-Kittel approach to the problem of oscillatory exchange coupling between ferromagnetic layers separated by a nonmagnetic metal spacer. This model provides a very simple explanation for the occurrence of long periods as well as multiperiodic oscillations, and is valid for arbitrary crystal structure and Fermi surface. The role of defects, such as misfit dislocations and interfacial roughness, is discussed.

I. INTRODUCTION

There is currently great interest in the exchange interaction between ferromagnetic layers separated by a nonmagnetic spacer layer. Among the most striking results is the reporting of a *multiperiodic* oscillatory coupling for the Fe/Cr/Fe(001) system:[1–3] here the superposition of short-period [$\Lambda \approx 2$ monolayers (ML's)] and long-period ($\Lambda \approx 10$–12 ML's) oscillations is observed. Similar results were also reported in Fe/Mn/Fe(001) (Ref. 4), Co/Cu/Co(001) (Ref. 5), and Fe/Au/Fe(001) (Ref. 6) systems.

The explanation of this spectacular phenomenon is a challenge to the theory. Some attempts have been made to calculate the exchange coupling as the total energy difference between the parallel and antiparallel configurations, either *ab initio*,[7–9] or within a tight-binding scheme.[10–12] Such calculations are quite difficult because the energy difference is several orders of magnitude smaller than the total energy itself. For this reason, total-energy calculations have been restricted to relatively small spacer thicknesses so far ($N \leq 6$ ML's and $N \leq 10$–20 ML's for *ab initio* and tight-binding calculations, respectively), and therefore appear not well suited for investigating long-period oscillatory coupling. Moreover, they often yield results that are at least one order of magnitude larger than experimental results,[7–9] so that the question of their numerical accuracy may be raised. Even if the problem of accuracy were removed, it might seem difficult, from total-energy calculations, to gain a simple intuitive picture of the physical mechanism involved in the coupling phenomenon.

On the other hand, the oscillatory behavior bears much resemblance with the one observed for Ruderman-Kittel-Kasuya-Yosida (RKKY) interactions between magnetic impurities. Thus the RKKY interaction appears a good candidate for the mechanism of oscillatory interlayer coupling. However, when applied in its simplest version (i.e., making a free-electron approximation and assuming a uniform continuous spin distribution within the ferromagnetic layers),[13,14] the RKKY theory predicts a single period $\Lambda = \lambda_F/2 \approx 1$ ML, which is much shorter than the experimental ones. It has been shown then that long periods can indeed be obtained within a simple RKKY theory, provided that the *discreteness* of the spacer thickness is taken into account.[15–17] In a recent paper[18] we have presented a general theory of RKKY interlayer exchange coupling; in this approach, the coupling is related in a physically transparent manner to the topological properties of the Fermi surface of the spacer material. Quantitative predictions were obtained for the oscillation periods in the case of noble-metal spacers.

The aim of the present paper is to give a more complete discussion of the ideas presented in Ref. 18. The model is introduced in Sec. II. For the sake of physical transparency, it is useful to first examine the implications of the RKKY model within the free-electron approximation; this is done in Sec. III, with special emphasis on the problem of multiperiodicity. It is often believed that multiperiodic oscillations are related to complicated Fermi surfaces; we show here that this belief is incorrect, and that multiperiodic oscillations may occur as well for systems with simple Fermi surfaces (for free electrons, for instance), provided that the *discrete* atomic structure within the ferromagnetic layers is considered. Section IV is devoted to a detailed description of the general theory sketched in Ref. 18. The influence of structural imperfections such as misfit dislocations and interfacial roughness is discussed in Sec. V. Finally, the results obtained for noble-metal spacers are given in Sec. VI and compared to recent experimental data.

II. MODEL

We consider two ferromagnetic monolayers $F1$ and $F2$ embedded in a nonmagnetic metal. The distance between $F1$ and $F2$ is $z = (N+1)d$, where d is the spacing between atomic planes and N the number of atomic planes of the spacer. The magnetic layers considered here consist of a single atomic layer, whereas those used for experimental studies are usually thicker; nevertheless, it has been found experimentally that the interlayer exchange coupling is roughly independent of the thickness of the magnetic layers, so that most of the coupling can be ascribed

to the outmost magnetic planes. Thus, as a first approximation, a model with monoatomic magnetic layers is expected to describe correctly the coupling phenomenon. The magnetic layers are assumed to consist of spins $\mathbf{S}_i$ located on the atomic positions $\mathbf{R}_i$ of the host metal. The magnetic layers are thus *coherent* with the spacer; this assumption plays an important role in the problem. It is expected to be relevant for epitaxially grown systems; deviations from this idealized situation will be discussed in Sec. V.

A magnetic layer (say $F1$) interacts with the conduction electrons of the host material and induces a spin polarization around it. This polarization is propagated accross the spacer and eventually interacts with $F2$, giving rise to an effective exchange interaction between $F1$ and $F2$. The problem of the exchange coupling between $F1$ anf $F2$ can thus be split into two aspects: (i) the interaction between a ferromagnetic layer and the host conduction electrons, and (ii) the way the spin polarization is propagated across the host material. For the case of transition-metal magnetic impurities, aspect (i) is usually ascribed to the so-called *s-d* mixing interaction.[19–21] Investigations of the interlayer exchange coupling on the basis of *s-d* mixing have been done by other authors;[22,23] this approach is rather sophisticated and relies mostly on numerical calculations, so that the results obtained so far are not very transparent; a detailed discussion of this aspect of the problem will be presented elsewhere.[24] In the present paper, we aim to focus on aspect (ii) of the problem, and in particular on the selection of the oscillation periods.

For this purpose, it is sufficient to approximate the coupling between the spins $\mathbf{S}_i$ and the conduction electrons (spin $\mathbf{s}$, position $\mathbf{r}$) by a contact potential

$$\mathcal{V}_i(\mathbf{r},\mathbf{s}) = A\,\delta(\mathbf{r}-\mathbf{R}_i)\;\mathbf{s}\cdot\mathbf{S}_i\;; \tag{1}$$

this is the form originally used by Ruderman and Kittel for investigating the indirect exchange coupling between nuclear spins,[25] and extended later by Kasuya[26] and Yosida.[27] The contact interaction (1), applied to transition-metal spins, is a rather crude approximation; it usually predicts incorrect phases for the oscillatory coupling, and the coupling strength is described by an adjustable parameter, A. These limitations of the RKKY model should be kept in mind when comparing its predictions with experimental results. On the other hand, it yields correct results for the oscillation periods, which are the quantities of interest here. Note that Schrieffer and Wolff[28] have shown that the *s-d* mixing approach is equivalent to the RKKY model in the limit of small *s-d* mixing parameter and large intra-atomic Coulomb repulsion, so that the limits of validity of the RKKY model are well defined.

The RKKY interaction between two spins $\mathbf{S}_i$ and $\mathbf{S}_j$ is[25,29]

$$\mathcal{H}_{ij} = J(\mathbf{R}_{ij})\;\mathbf{S}_i\cdot\mathbf{S}_j\;, \tag{2}$$

where the exchange integral is

$$J(\mathbf{R}_{ij}) = -\frac{1}{2}\left(\frac{A}{V_0}\right)^2\frac{V_0}{(2\pi)^3}\int d^3\mathbf{q}\;\chi(\mathbf{q})\exp(i\mathbf{q}\cdot\mathbf{R}_{ij})\;, \tag{3}$$

V_0 is the atomic volume and

$$\chi(\mathbf{q}) = \frac{V_0}{(2\pi)^3}\sum_{n,n'}\int d^3\mathbf{k}\;\frac{f(\epsilon_{n,\mathbf{k}})-f(\epsilon_{n',\mathbf{k}+\mathbf{q}+\mathbf{G}})}{\epsilon_{n',\mathbf{k}+\mathbf{q}+\mathbf{G}}-\epsilon_{n,\mathbf{k}}} \tag{4}$$

is the nonuniform susceptibility of the host material (in units of $2\mu_B^2$/atom). These expressions are given within a *reduced zone scheme*: the integration over $\mathbf{q}$ and $\mathbf{k}$ in Eqs. (3) and (4), respectively, is performed within the first Brillouin zone (FBZ), and the indices n and n' refer to the energy bands; $\mathbf{G}$ is a vector of the reciprocal lattice chosen such that $\mathbf{k}+\mathbf{q}+\mathbf{G}$ belongs to the FBZ. The interlayer coupling is obtained from (3) and (4) by summing $\mathcal{H}_{ij}$ over all the pairs ij, i and j running respectively on $F1$ and $F2$. The coupling energy per unit area can be written

$$E_{1,2} = I_{1,2}\cos\theta_{1,2}\;, \tag{5}$$

where $\theta_{1,2}$ is the angle between the magnetizations of $F1$ and $F2$. The interlayer coupling constant $I_{1,2}$ is given by

$$I_{1,2} = \frac{d}{V_0}S^2\sum_{j\in\mathrm{F2}}J(\mathbf{R}_{Oj})\;, \tag{6}$$

where O labels one site of $F1$ taken as the origin. Note that within the present sign convention, positive (negative) values of $I_{1,2}$ correspond to antiferromagnetic (ferromagnetic) coupling.

III. FREE-ELECTRON APPROXIMATION

Before attempting to calculate the coupling in a general case, it is instructive to first examine it within the free-electron approximation. The calculations can then be performed in an almost completely analytical manner so that the results are physically transparent; moreover, many features of the coupling thus obtained remain qualitatively valid in more realistic situations. In all this section, the host material will be approximated by a free-electron gas with the same density; since the model will be applied to noble metals in this paper, we consider fcc host materials with one conduction electron per atomic cell, so that the Fermi vector is $k_F = (12\pi^2)^{1/3}/a$, where a is the lattice parameter. The spins $\mathbf{S}_i$ are still supposed to be located on the atomic sites of the fcc lattice. In this section, we adopt the point of view of an *extended zone scheme*, which provides the most natural description for a free-electron gas. Thus, the integrals over $\mathbf{q}$ and $\mathbf{k}$ in Eqs. (3) and (4) extend to infinity.[29] To avoid any confusion, the susceptibility is noted here $\bar{\chi}(\mathbf{q})$. The exchange integral in the free-electron approximation is given by the well-known expression[25]

$$J(\mathbf{R}) = \frac{4A^2mk_F^4}{(2\pi)^3\hbar^2}\,F(2k_FR)\;, \tag{7a}$$

with

$$F(x) = \frac{x\cos x - \sin x}{x^4} \approx \frac{\cos x}{x^3} \quad \text{for } x \to +\infty ; \tag{7b}$$

it oscillates with a period $\Lambda = \lambda_F/2$ and decays as R^{-3}.

As a first approximation, one may try to replace the actual ferromagnetic layers by a continuous uniform distribution of spins with the same spin density, i.e., we perform in Eq. (6) the substitution

$$\sum_{F2} \longrightarrow \frac{d}{V_0}\int_{F2} d^2\mathbf{R}_\parallel . \tag{8}$$

In the above equation, $\mathbf{R}_\parallel$ is the in-plane projection of $\mathbf{R}_{Oj}$. The interlayer coupling is then given as a function of the distance z by

$$I_{1,2}(z) \approx -I_0 \frac{d^2}{z^2}\sin(2k_F z) \quad \text{for } z \to \infty , \tag{9a}$$

with

$$I_0 = \left(\frac{A}{V_0}\right)^2 S^2 \frac{m}{16\pi^2\hbar^2} . \tag{9b}$$

There is a single oscillation period $\Lambda = \lambda_F/2$, and the coupling decays as z^{-2}; this result was first obtained by Yafet.[13]

A. Multiperiodicity

We want now to examine the validity of the continuous approximation (8). When performing the continuous integration (8) over $F2$, the integrand is a function of $\mathbf{R}_\parallel$, which oscillates with a period of the order of $\lambda_F/2$; thus if the inter-atomic distance b within the plane is smaller than $\lambda_F/2$ we may expect the continuous approximation (8) to be valid. On the other hand, if b is large as compared to $\lambda_F/2$, it is clear that approximation (8) must break down.

In order to develop this argument in a more quantitative fashion, we perform explicitly the summation (6) without making the continuous approximation (8):

$$I_{1,2}(z) = -\frac{1}{2}\left(\frac{A}{V_0}\right)^2 S^2 \frac{d}{(2\pi)^3}\int_{-\infty}^{+\infty} dq_z \exp(iq_z z)\int d^2\mathbf{q}_\parallel \bar{\chi}(\mathbf{q}_\parallel, q_z) \sum_{\mathbf{R}_\parallel \in F2} \exp(i\mathbf{q}_\parallel \cdot \mathbf{R}_\parallel) . \tag{10}$$

Because of the translational invariance in the layer plane, the last sum in the above equation is zero unless $\mathbf{q}_\parallel$ is a vector $\mathbf{G}_\parallel$ belonging to the (two-dimensional) reciprocal lattice of $F2$. Thus the expression of the coupling becomes

$$I_{1,2}(z) = -\frac{1}{2}\left(\frac{A}{V_0}\right)^2 S^2 \frac{d}{V_0}\frac{d}{2\pi} \times \sum_{\mathbf{G}_\parallel}\int_{-\infty}^{+\infty} dq_z \exp[i(q_z z + \mathbf{G}_\parallel \cdot \mathbf{R}_\parallel^0)] \times \bar{\chi}(\mathbf{G}_\parallel, q_z) , \tag{11}$$

where $\mathbf{R}_\parallel^0$ is the in-plane displacement needed to bring $F2$ into coincidence with $F1$; the associated phase shift $\mathbf{G}_\parallel \cdot \mathbf{R}_\parallel^0$ depends on N. As is well known, the susceptibility $\bar{\chi}(\mathbf{q})$ depends only on q and has a logarithmic singularity in its derivative at $q = 2k_F$ (Kohn singularity), which is responsible for the long-range oscillatory behavior of the exchange coupling. Thus, the contribution to $I_{1,2}(z)$ corresponding to a given vector $\mathbf{G}_\parallel$ gives a long-range oscillatory interlayer coupling if, when integrating over q_z, one crosses a singularity, i.e., if $G_\parallel < 2k_F$; the corresponding wave vector is $[(2k_F)^2 - G_\parallel^2]^{1/2}$.

It is clear from the above discussion that the multiperiodicity is related to the discrete atomic structure within the layers, and that the number of oscillation periods increases as the in-plane atomic density decreases. This trend is well exemplified for the case of a fcc spacer: as shown in Fig. 1, the number of different oscillation periods for the (111), (001), and (110) orientations is, respectively, 1, 2, and 3.

For a vector $\mathbf{G}_\parallel \neq \mathbf{0}$, it is easily shown that the strength of the singularity is reduced by a factor $[1 - (G_\parallel/2k_F)^2]^{1/2}$. Thus the expression of the interlayer coupling in the limit of large thicknesses is

$$I_{1,2}(z) \approx -I_0 \frac{d^2}{z^2}\sum_{G_\parallel < 2k_F}\left[1 - \left(\frac{G_\parallel}{2k_F}\right)^2\right]^{1/2} \times \sin\{[(2k_F)^2 - G_\parallel^2]^{1/2} z + \mathbf{G}_\parallel \cdot \mathbf{R}_\parallel^0\} . \tag{12}$$

Note that, as stressed above, the phase $\mathbf{G}_\parallel \cdot \mathbf{R}_\parallel^0$ depends on N; this must be considered to evaluate the oscillation period from Eq. (12).

B. Aliasing

At first sight, the prediction of a period $\lambda_F/2$ much shorter than any observed period might seem to invalidate the RKKY mechanism. Actually, it has been pointed out by several authors[15–17] that this apparent discrepancy can be removed by a very simple argument: the spacer thickness $z = (N+1)d$ (with N an integer) is not a continuous variable so that an *effective period* much larger than $\lambda_F/2$ may result from this discrete sampling.

This effect, known as *aliasing*, is well understood from the theory of Fourier analysis: let $f(z)$ be a function of a continuous variable z, characterized by its Fourier transform $F(q)$; if f_N is a series obtained by sampling f at equally spaced intervals [i.e., $f_N \equiv f(z = Nd)$ with N integer], the Fourier representation $\tilde{F}(q)$ of f_N is peri-

odic of period $2\pi/d$. Thus, values of q in the interval $[-\pi/d;\pi/d]$ are sufficient to describe f_N, and $\tilde{F}(q)$ is obtained from $F(q)$ by folding it into $[-\pi/d;\pi/d]$

$$\tilde{F}(q) = \sum_{n=-\infty}^{+\infty} F(q + 2\pi n/d) \ . \tag{13}$$

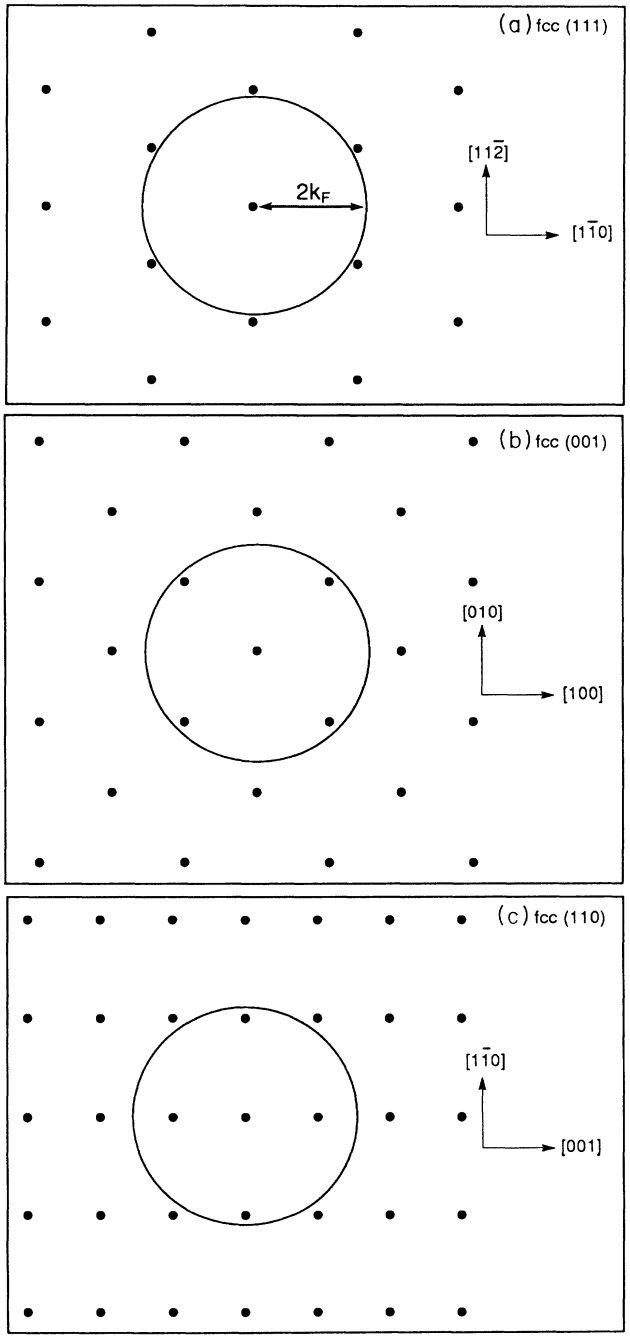

FIG. 1. Two-dimensional reciprocal lattice for fcc layers; (a), (b), and (c) correspond, respectively, to the (111), (100), and (110) orientations. The sphere of radius $2k_F$ is the locus of singularities of the susceptibility $\chi(\mathbf{q})$; it should not be confused with a Fermi sphere. The unit vectors have a length $2\pi/a$.

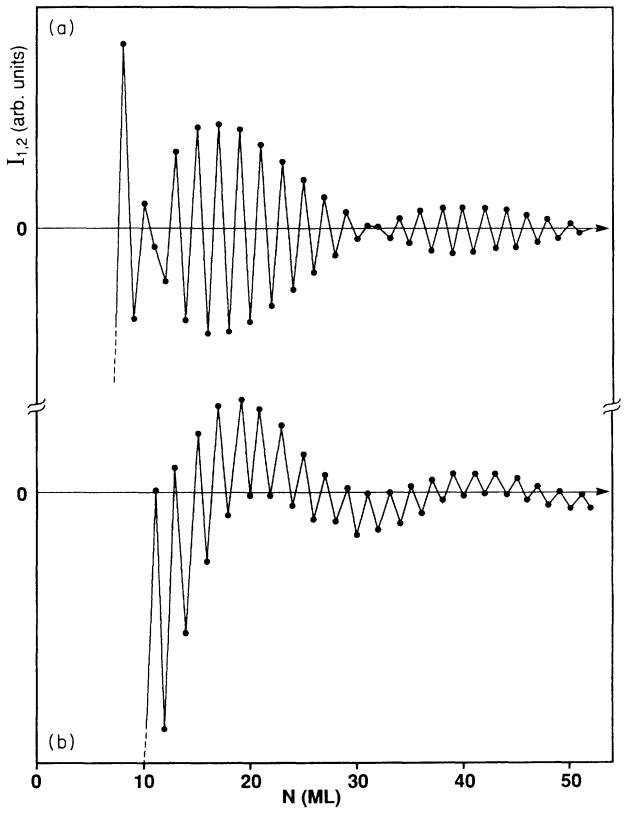

FIG. 2. (a) Oscillatory coupling with a single period $\Lambda = 2.1$ ML's, showing the modulation of period 21 ML's due to the beat phenomenon. (b) Oscillatory coupling with two different periods: $\Lambda_1 = 2$ ML's and $\Lambda_2 = 21$ ML's.

Actually, the choice of the q interval is arbitrary: any interval of length $2\pi/d$ would give equivalent results; the interval $[-\pi/d;\pi/d]$ represents the best choice, since periods smaller than $2d$ are physically meaningless.

Thus the *effective period* Λ associated to a given q vector is given by

$$\frac{2\pi}{\Lambda} = \left| q - n\frac{2\pi}{d} \right| \ , \tag{14}$$

where n is chosen such that $\Lambda > 2d$. In addition to the aliasing effect, a *beat* phenomenon may arise from the incommensurability of Λ and d: if Λ is close to an integer number P of monolayers (say $\Lambda/d = P + x$), then the envelope of the oscillations is modulated with a period $\Lambda/|x|$, as shown in Fig. 2(a). This beat phenomenon should not be confused with the superposition of a long-period oscillation [Fig. 2(b)]. However, if only the antiferromagnetic part of the coupling is detected, as is often the case, it might be difficult in practice to distinguish between these two different behaviors.

IV. GENERAL THEORY

A. Calculation of the coupling

Our starting point is the expression of the interlayer coupling as given by Eqs. (3)–(6). Here and in the follow-

ing, we consider for simplicity a single conduction band; the generalization to several bands is immediate.[29] The integrals over $\mathbf{q}$ and $\mathbf{k}$ in Eqs. (3) and (4), respectively, are performed over the FBZ. This is not well adapted to the symmetry of our problem. Thus we define all the functions of $\mathbf{q}$ and $\mathbf{k}$ outside the FBZ by repeating them periodically on the reciprocal lattice. In other words, we use a *periodic zone scheme*, which yields a completely equivalent description; this allows us to leave out the reciprocal lattice vector $\mathbf{G}$ in Eq. (4). Now, the integration can be performed on any elementary cell of the reciprocal space; the convenient choice is a unit cell of prismatic shape as shown in Fig. 3: the in-plane components $\mathbf{q}_\parallel$ and $\mathbf{k}_\parallel$ run over the two-dimensional FBZ (2DBZ) of the layers, whereas q_z and k_z run from $-\pi/d$ to π/d. The advantage of using the prismatic auxilliary zone instead of the FBZ is that the integration over the z and in-plane components of the wave vector can be separated. The expression of the coupling becomes

$$I_{1,2} = -\frac{1}{2}\left(\frac{A}{V_0}\right)^2 S^2 \frac{d}{(2\pi)^3}\int_{-\pi/d}^{\pi/d} dq_z\, e^{iq_z z}\int_{\mathrm{2DBZ}} d^2\mathbf{q}_\parallel\, \chi(\mathbf{q}_\parallel, q_z) \sum_{\mathbf{R}_\parallel \in \mathrm{F2}} \exp(i\mathbf{q}_\parallel\cdot\mathbf{R}_\parallel)\ . \tag{15}$$

Now, the last sum in the above equation is zero unless $\mathbf{q}_\parallel = \mathbf{0}$ (the only vector $\mathbf{G}_\parallel$ belonging to the 2DBZ), so that, as pointed out by Yafet,[30] the interlayer coupling is given by the (one-dimensional) Fourier transform of the susceptibility $\chi(q_z) \equiv \chi(\mathbf{q}_\parallel = \mathbf{0}, q_z)$:

$$I_{1,2} = -\frac{1}{2}\left(\frac{A}{V_0}\right)^2 S^2 \frac{d}{V_0}\frac{d}{2\pi}\int_{-\pi/d}^{\pi/d} dq_z\, \chi(q_z)\, e^{iq_z z}\ , \tag{16}$$

which can be written

$$I_{1,2} = -\left(\frac{A}{V_0}\right) S^2 \frac{d^2}{32\pi^4}\int_{\mathrm{2DBZ}} d^2\mathbf{k}_\parallel\, B(\mathbf{k}_\parallel) \tag{17a}$$

with

$$B(\mathbf{k}_\parallel) = \int_{-\pi/d}^{\pi/d} dk_z \int_{-\pi/d}^{\pi/d} dk_z'\, \frac{f(\epsilon_{\mathbf{k}_\parallel,k_z}) - f(\epsilon_{\mathbf{k}_\parallel,k_z'})}{\epsilon_{\mathbf{k}_\parallel,k_z'} - \epsilon_{\mathbf{k}_\parallel,k_z}} \times e^{i(k_z'-k_z)z}\ , \tag{17b}$$

where we have changed the variable q_z for k_z'. Note that, in contrast to the preceeding section (where a different point of view was adopted), only $\mathbf{G}_\parallel = \mathbf{0}$ contributes; here multiperiodicity arises from the multiple singularities of $\chi(\mathbf{q}_\parallel = \mathbf{0}, q_z)$. This is because the *periodic zone scheme* (in contrast to the *extended zone scheme*) folds all the reciprocal lattice vectors $\mathbf{G}$ onto $\mathbf{G} = \mathbf{0}$.

To evaluate $B(\mathbf{k}_\parallel)$, we proceed as in Ref. 29: noting that the most important contributions come from states close to the Fermi surface, we expand $\epsilon_{\mathbf{k}_\parallel,k_z}$ and $\epsilon_{\mathbf{k}_\parallel,k_z'}$ around ϵ_F to first order in k_z and k_z'; next we change k_z and k_z' for energy variables ϵ and ϵ' and perform the integrations over ϵ and ϵ' by using complex-contour-integration techniques. Thus we get

$$B(\mathbf{k}_\parallel) = \frac{2\pi}{z}\sum_{\mu,\nu}\frac{e^{iq_z^{\mu,\nu}z}}{\hbar\,(|v_z^\mu| + |v_z^\nu|)}\, F_{\mu,\nu}(z,T) + \text{c.c.} \tag{18}$$

In the above equation, $q_z^{\mu,\nu} = k_z^\mu - k_z^\nu$, where k_z^μ (k_z^ν) is such that $\epsilon_{\mathbf{k}_\parallel,k_z^\mu} = \epsilon_F$ ($\epsilon_{\mathbf{k}_\parallel,k_z^\nu} = \epsilon_F$) and the z component of the velocity $v_z^\mu > 0$ ($v_z^\nu < 0$), as sketched in Fig. 4. It is also useful to introduce an effective velocity: $v_z^{\mu,\nu} = 2|v_z^\mu v_z^\nu|/(|v_z^\mu| + |v_z^\nu|)$. The function $F_{\mu,\nu}(z,T)$ describes the temperature dependence of $B(\mathbf{k}_\parallel)$ due to the rounding of the Fermi-Dirac function $f(\epsilon)$:

$$F_{\mu,\nu}(z,T) = \frac{z/L_{\mu,\nu}(T)}{\sinh\left(z/L_{\mu,\nu}(T)\right)}\ , \tag{19}$$

where $L_{\mu,\nu}(T)$ is an attenuation length given by

$$L_{\mu,\nu}(T) = \frac{\hbar v_z^{\mu,\nu}}{2\pi k_B T}\ . \tag{20}$$

Next we proceed with the integration over $\mathbf{k}_\parallel$. As $\mathbf{k}_\parallel$ varies, the factor $\exp(iq_z^{\mu,\nu}z)$ oscillates very rapidly, so that only the neighborhood of the vectors $\mathbf{k}_\parallel^\alpha$ for which

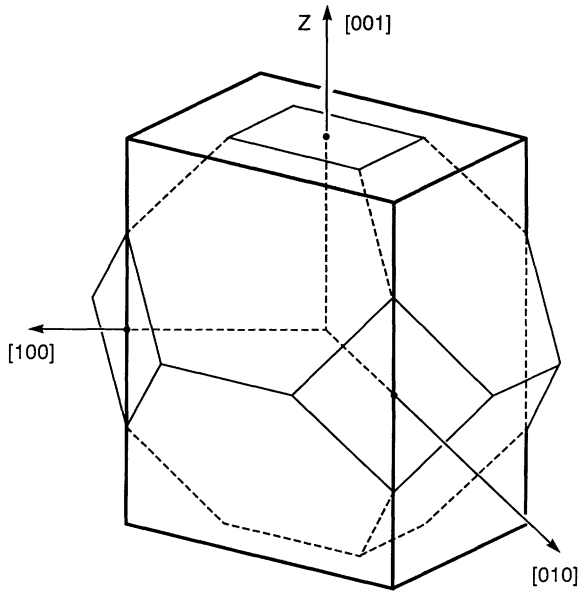

FIG. 3. First Brillouin zone of the fcc lattice (thin lines), and auxiliary zone for the (001) orientation (bold lines).

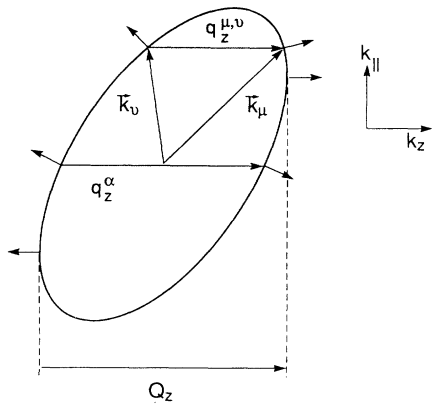

FIG. 4. Sketch showing the wave vector $q_z^{\mu,\nu}$ and the stationary vector q_z^α. The calliper Q_z of Roth, Zeiger, and Kaplan (Ref. 29) is also shown. The small arrows are the velocity vectors. See text for further explanations.

$q_z^{\mu,\nu}$ is stationary contribute to the integral. In the following, the index α specifies such a stationary point, and will be used instead of (μ,ν) for all quantities taken at this point. It is easily seen that such stationary points correspond to vectors q_z^α linking two points of the Fermi surface with antiparallel velocities, as shown on Fig. 4.[18]

The integral can be calculated by using the stationary phase approximation: $\mathbf{k}_\parallel$ is kept constant, equal to $\mathbf{k}_\parallel^\alpha$, except in the phase factor, and $q_z^{\mu,\nu}$ is expanded to second order in $\mathbf{k}_\parallel - \mathbf{k}_\parallel^\alpha$, i.e.,

$$q_z^{\mu,\nu} = q_z^\alpha + \frac{(k_x - k_x^\alpha)^2}{\kappa_x^\alpha} + \frac{(k_y - k_y^\alpha)^2}{\kappa_y^\alpha} , \tag{21}$$

where the cross terms have been cancelled by an appropriate rotation of the x and y axes; κ_x^α and κ_y^α defined above are the *combined* principal curvature radii of the Fermi surface for the stationary vector q_z^α. We also define the effective mass m_α^*, and the phase ψ_α by

$$m_\alpha^* = \frac{2\hbar\,|\kappa_x^\alpha \kappa_y^\alpha|^{1/2}}{|v_z^\mu| + |v_z^\nu|} , \tag{22}$$

and

$$\psi_\alpha = \frac{\pi}{2} + \frac{\pi}{4}\left[\mathrm{sgn}(\kappa_x^\alpha) + \mathrm{sgn}(\kappa_y^\alpha)\right] ; \tag{23}$$

ψ_α is, respectively, equal to 0, $\pi/2$, and π when q_z^α is a maximum, a saddle point, and a minimum.

We finally obtain for the interlayer coupling

$$I_{1,2}(z) = -I_0 \frac{d^2}{z^2} \sum_\alpha \frac{m_\alpha^*}{m} \sin(q_z^\alpha + \psi_\alpha)\, F_\alpha(z,T) , \tag{24}$$

where I_0 is the same as in Eq. (9). As already discussed extensively, if $q_z^\alpha > \pi/d$, we must add or substract $2\pi/d$, in order to bring it into the interval $[-\pi/d;\pi/d]$. The oscillation periods are $\Lambda_\alpha = 2\pi/|q_z^\alpha|$. The sign of q_z^α is positive (negative), when q_z^α is "inside" ("outside"), as shown on Fig. 5.[31]

B. Effect of nesting

The result expressed by Eq. (24) holds if κ_x^α and κ_y^α are not infinite. If both κ_x^α and κ_y^α are infinite, then the two parts of the Fermi surface linked by q_z^α closely fit each other, up to second order in $(\mathbf{k}_\parallel - \mathbf{k}_\parallel^\alpha)$: this case will be referred to as *complete nesting*. If only one of the combined principal curvature radii is infinite, the two parts of the Fermi surface fit each other along a line: this case is referred to as *partial nesting*.

The nesting has a dramatic effect, for it changes the exponent in the power-law decrease of the oscillatory coupling. For partial and complete nesting, we find that the coupling decreases as $z^{-3/2}$ and z^{-1}, respectively, instead of z^{-2} in the usual case. Therefore, the interlayer coupling has a much longer range in the case of nesting.

This effect is relevant to the case of Fe/Cr/Fe(001). The short period ($\Lambda \approx 2$ ML's) observed for this system[1-3] has been interpreted as associated with a vector $|q_z^\alpha| = 0.95\,\Gamma H$.[22] This vector yields an almost perfect nesting of the electron and hole pockets of the Cr Fermi surface, respectively, around the points Γ and H of the bcc FBZ, which is believed to be responsible for the spin-density-wave antiferromagnetism of Cr. Thus, our analysis of the effect of nesting provides a sensible explanation for the very slow decrease of the short-period oscillatory coupling in Fe/Cr/Fe(001), which has been observed up to Cr thicknesses as large as 50 ML's.[32]

C. Magnetic planes versus magnetic impurities

The theory of RKKY interaction between isolated magnetic impurities for a nonspherical Fermi surface was first given by Roth, Zeiger, and Kaplan.[29] The problem discussed here (interaction between magnetic planes)

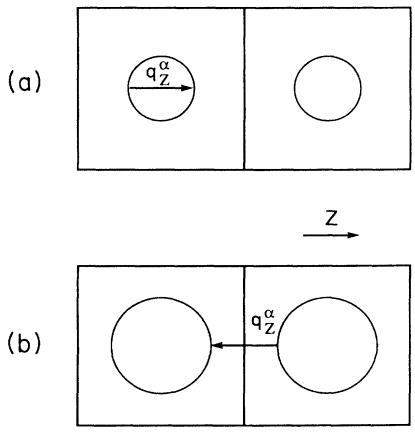

FIG. 5. Sketch explaining the sign convention for q_z^α. (a) q_z^α is "inside" the Fermi surface, i.e., positive; (b) q_z^α is "outside" the Fermi surface, i.e., negative.

presents many features similar to the one studied by Roth, Zeiger, and Kaplan, and also significant differences. It is instructive to compare the two situations.

In the theory of Roth, Zeiger, and Kaplan, the exchange interaction between two spins $\mathbf{S}_i$ and $\mathbf{S}_j$ oscillates with periods given by the callipers Q_z of the Fermi surface along the z direction (taken parallel to the ij axis), as shown on Fig. 4, i.e., by the z projection of vectors $\mathbf{Q}$ linking two points of the Fermi surface having their velocity, respectively, parallel and antiparallel to z, but the vectors $\mathbf{Q}$ themselves must not be parallel to z. On the contrary, as discussed above, the oscillation periods of the interlayer coupling are given by stationary vectors q_z^α, i.e., by vectors parallel to z, which link two points of the Fermi surface with antiparallel velocities; the velocities themselves may be at an arbitrary angle γ_α with respect to the z axis (see Fig. 4).

In both cases the strength of the coupling involves an effective mass related to the curvature radii of the Fermi surface. The temperature dependence has the same form (19), with an attenuation length inversely proportional to T and depending on the Fermi velocities. Also, the phase of the oscillations is related in both cases to the topological nature of the q_z^α (Q_z): maximum, minimum, or saddle point.

V. INFLUENCE OF STRUCTURAL IMPERFECTIONS

A. Influence of misfit dislocations

So far we have considered only systems with perfectly ordered structures. While it is obvious that real systems always present some defects, it is of crucial importance to evaluate the influence of departures from the hypothetical perfect systems. Among the defects that play an important role in ultrathin films are the misfit dislocations. They occur when the lattice parameter of a layer does not match exactly the one of the underlying layer, which is a very frequent situation. Assuming that the mismatch is entirely accommodated by interfacial dislocations, the average distance between the dislocations is approximately $D \approx d/|\eta|$, where η is the lattice mismatch between the magnetic material and the spacer material (we neglect here the difference between the in-plane lattice parameter b and the interplane distance d, which is unimportant for the qualitative discussion given here).

The effect of the dislocations is to destroy the in-plane translational symmetry for distances larger than D. Because of the loss of translational invariance, $\mathbf{q}_\parallel$ is no longer exactly equal to zero in Eq. (15); instead, it is distributed around zero with a typical width $\Delta q_\parallel \approx 1/D$. One can easily see that this distribution of $\mathbf{q}_\parallel$ in turn induces a distribution of the stationary vectors q_z^α of typical width $\Delta q_z^\alpha \approx \Delta q_\parallel \tan\gamma_\alpha$ (to first order in $\Delta q_\parallel$), where γ_α is the angle between the corresponding Fermi velocity and the z direction (see Fig. 4). Because of the distribution of q_z^α, the coupling will be rapidly suppressed by destructive interferences for z larger than $z_{\max}^\alpha \approx 1/\Delta q_z^\alpha \approx D/\tan\gamma_\alpha$, i.e.,

$$z_{\max}^\alpha \approx \frac{d}{|\eta| \tan\gamma_\alpha} \tag{25}$$

The cutoff distance $z_{\max}^\alpha$ is thus small when the angle γ_α is large. This result may be interpreted by the following simple picture: because of the loss of translational invariance, the electrons have a finite in-plane coherence length ($\approx D$); since the electrons that carry the coupling have a velocity at an angle γ_α with respect to the z axis, the coherence length in the z direction is $\approx D/\tan\gamma_\alpha$. The cutoff distances $z_{\max}^\alpha$ corresponding to the various periods will in general be different, since the angles γ_α themselves may be different.

For a noble-metal spacer in the (001) orientation the angle γ_α is zero for the two periods, whereas in the (111) orientation it is very large ($\gamma_\alpha = 62°$–$68°$). Thus we expect the coupling to be rather insensitive to the misfit dislocations for the (001) orientation, whereas the effect should be dramatic for the (111) orientation. To be more quantitative, we have evaluated the cutoff length for Cu/Co/Cu(111) and Au/Co/Au(111), where the mismatch is, respectively, $|\eta| = 2.5\%$ and $|\eta| = 14\%$: the estimated cutoff length is, respectively, $z_{\max}^\alpha \approx 25$ ML's and $z_{\max}^\alpha \approx 4$ ML's.

B. Influence of interfacial roughness

The term *roughness* is a very vague one. Thus, it seems important to give a precise (as far as possible) definition of what is meant by roughness. Let z_1 and z_2 be the position of the interfaces bounding the spacer layer. Because of the imperfect growth mode, they are not constant over the layer, but fluctuate as a function of $\mathbf{R}_\parallel$. We need at least two parameters to describe these fluctuations. The first one is the width σ of the distribution for z_1 and z_2 (which we may assume to be the same for the two interfaces). The second parameter is the lateral correlation length for the fluctuations of z_1 and z_2; we may roughly describe it as the average "diameter" ξ of the flat portions of the interfaces. Another important characteristic of the problem is the degree of mutual correlation of the two interfaces.

It is not possible to give a rigorous description of the influence of roughness on the interlayer coupling, so that we must rely on qualitative arguments. Basically, we may expect the effect of roughness to be twofold: (i) it causes the spacer thickness z to fluctuate with an amplitude Δz around its average value $\bar{z}$, so that the coupling must be averaged over these thickness fluctuations and (ii) it breaks the in-plane translational invariance over distances larger than ξ.

Effect (ii) is completely analogous to the effect of misfit dislocations discussed above, so that it causes the coupling to be suppressed for spacer thicknesses larger than

$$z_{\max}^\alpha \approx \frac{\xi}{\tan\gamma_\alpha} . \tag{26}$$

This effect has been overlooked by Wang, Levy, and Fry in their discussion of roughness.[22]

The effect (i) can be described by convoluting $I_{1,2}(z)$

with the distribution of thickness fluctuations $P(z-\bar{z})$, or equivalently by multiplying $\chi(q_z)$ by the Fourier transform $\tilde{P}(q_z)$ of $P(z-\bar{z})$ in Eq. (16). This is the formulation used by Wang, Levy, and Fry.[22] If the two interfaces are mutually *uncorrelated* (as was implicitely assumed in Ref. 22), then $\tilde{P}(q_z)=\tilde{P}_1(q_z)\tilde{P}_2(q_z)$, i.e., $\Delta z=\sqrt{2}\,\sigma$ (for Gaussian distributions); however, if the two interfaces are mutually *correlated* the latter relation no longer holds, and Δz may be much smaller than $\sqrt{2}\,\sigma$. The effect of the thickness fluctuations is basically to smooth out oscillations with a period shorter than Δz, i.e., it acts as a low-pass filter for the oscillation frequency. This effect is well exemplified for a Cu (001) spacer in Fig. 2 of Ref. 18. It is responsible for the absence of the short-period oscillation ($\Lambda\approx 2$ ML's) in Fe/Cr/Fe(001) when the layers are not atomically smooth.[1–3]

It is important to note that the coupling is influenced in a completely different manner by effects (i) and (ii): (i) influences the oscillatory coupling according to its period, whereas (ii) affects oscillations corresponding to large values of γ_α, independently of their period.

C. Influence of strain

Strain is a common feature of multilayers. A homogeneous strain may arise, for instance, from the interfacial lattice mismatch between the different materials.[33] Strictly speaking, a homogeneous strain is not a defect, but merely a modification of the structure. Nevertheless, it is expected to modify the Fermi surface with respect to the bulk and hence also the periods of oscillatory coupling. As discussed in Ref. 34, the modification of the Fermi surface depends crucially on the kind of strain, and for a given strain the change in period will depend on the kind of stationary vector q_z^α. Moreover, in real films, one can expect the strain to be thickness dependent and anisotropic.

To treat this effect thoroughly would require band-structure calculations, which is beyond our present purpose. One can nevertheless obtain a rough estimate the magnitude of the effect from published experimental results, in the simple case of an isotropic volume strain $\Delta V_0/V_0$ in Cu.[34] These de Haas–van Alphen results are given in terms of the cross-sectional area $\mathcal{A}$ of closed stationary orbit around the Fermi surface: the belly $<001>$ and the "neck" orbits change, respectively, as $d\ln\mathcal{A}/d\ln V_0\approx -0.6$ and $d\ln\mathcal{A}/d\ln V_0\approx -3$. As shown in Ref. 18 the "diameter" of these orbits is related to the long-period oscillation ($\Lambda_2=5.9$ ML's) for the (001) orientation and the oscillation period ($\Lambda=4.5$ ML's) for the (111) orientation, respectively. Thus we expect the latter to be much more strain-sensitive than the former (roughly by a factor 5). Moreover, even larger changes of the "neck" orbit are reported for anisotropic strains.[34]

VI. RESULTS FOR NOBLE METALS

Among the different metals that have been used as spacers in sandwiches and multilayers, the noble metals are those that possess the simplest Fermi surface. Furthermore, their Fermi surface properties are known with a very high accuracy from de Haas–van Alphen and cyclotron resonance experiments.[35] They appear therefore as prototype systems to test the predictions of the RKKY theory. This has been done for Cu, Ag, and Au in (111), (001), and (110) orientations in Ref. 18 by using experimental Fermi surface data from Ref. 35. For both noble metals, the number of different oscillation periods is, respectively, 1, 2, and 4 for (111), (100), and (110) orientations, so that the trend obtained within the free-electron approximation for the number of periods versus the in-plane atomic density remains valid.

Since the publication of our previous paper,[18] some new experimental results have become available. A comparison between the theoretically predicted periods and those that have been observed so far is given in Table I.

For Cu (111), the observed period[36–38] is somewhat larger than the predicted one; however, the difference

TABLE I. Comparison between the oscillation periods predicted by the RKKY theory (Ref. 18) for noble metals and those observed experimentally.

Spacer	Theoretical periods	System	Experimental periods	Ref.
		Co/Cu/Co	$\Lambda\approx 6$ ML's	36
Cu (111)	$\Lambda=4.5$ ML's	Co/Cu/Co	$\Lambda\approx 5$ ML's	37
		Fe/Cu/Fe	$\Lambda\approx 6$ ML's	38
		Co/Cu/Co	$\Lambda\approx 6$ ML's	39
Cu (001)	$\Lambda_1=2.6$ ML's $\Lambda_2=5.9$ ML's	Fe/Cu/Fe	$\Lambda\approx 7.5$ ML's	40
		Co/Cu/Co	$\Lambda_1\approx 2.6$ ML's $\Lambda_2\approx 8$ ML's	5
Au (001)	$\Lambda_1=2.6$ ML's $\Lambda_2=8.6$ ML's	Fe/Au/Fe	$\Lambda_1\approx 2$ ML's $\Lambda_2\approx 7$–8 ML's	6

is not dramatic and may be attributed to experimental incertainties, and/or to the strain effect mentioned above.

The (001) orientation is of particular interest, since our RKKY theory predicts the existence of both a short and a long period. For Cu (001), the two periods have been actually found,[5] whereas some authors observed only the long period.[39,40] The absence of the short period here may be due to the roughness, as discussed above. The agreement between the theoretical and experimental periods is rather good. For Au (001) the comparison is even better: the two periods have been found,[6] in close agreement with the theoretical predictions.

The results displayed in Table I clearly show that the RKKY theory allows to predict in an essentially correct manner the periods of oscillatory interlayer coupling, simply by inspection of the Fermi surface of the spacer metal. In particular, the observation of the two periods predicted for Cu (001) and Au (001) is a clear confirmation of our statement that multiperiodicity is not necessarily related to complicated Fermi surfaces, but can occur as well in systems with comparatively simple Fermi surfaces (like noble metals), for crystallographic orientations of low in-plane atomic density.

VII. CONCLUSION

We have given a comprehensive discussion of the implications of the RKKY model for the coupling between ferromagnetic layers separated by a nonmagnetic spacer. We show in particular the connection between the multiperiodicity of coupling oscillations and the discreteness of the spin distribution within the ferromagnetic layers. Our results are quite general and allow us, in principle, to predict the oscillation periods for any spacer metal in any crystallographic orientation, knowing only its Fermi surface. We have applied this model to the noble metals, whose Fermi surface are well known: the overall agreement is excellent, at least with recent results on high-quality samples. We have also given a schematic theory of the influence of structural imperfections in real films, which can explain some puzzling experimental results.

However, the basic assumption of the RKKY theory, a contact-type interaction between the magnetic moments and the conduction electrons, is not appropriate for ferromagnetic $3d$ transition metals. As a consequence, the present model is unable to describe correctly the intensity and the phase of the coupling oscillations. To this purpose, one needs to treat in an explicit manner the hybridization between the $3d$ bands of the ferromagnetic metal and the conduction band of the spacer metal. This will be treated in a forthcoming paper.[24]

ACKNOWLEDGMENT

The Institut d'Electronique Fondamentale is Unité Associée No. 22 au Centre National de la Recherche Scientifique.

---

*Presently on leave at the IBM Almaden Research Center, K32-802, 650 Harry Road, San Jose, CA 95120-6099.

[1] J. Unguris, R.J. Celotta, and D.T. Pierce, Phys. Rev. Lett. **67**, 140 (1991).
[2] S.T. Purcell, W. Folkerts, M.T. Johnson, N.W.E. McGee, K. Jager, J. aan de Stegge, W.B. Zeper, W. Hoving, and P. Grünberg, Phys. Rev. Lett. **67**, 903 (1991).
[3] S. Demokritov, J.A. Wolf, P. Grünberg, and W. Zinn, in *Magnetic Thin Films, Multilayers and Surfaces*, edited by S.S.P. Parkin, H. Hopster, J.P. Renard, T. Shinjo, and W. Zinn, Materials Research Society Proceedings Series (Materials Research Society, Pittsburgh, 1992), Vol. 231, p. 133.
[4] S.T. Purcell, M.T. Johnson, N.W.E. McGee, R. Coehoorn, and W. Hoving, Phys. Rev. B **45**, 13 064 (1992).
[5] M.T. Johnson, S.T. Purcell, N.W.E. McGee, R. Cochoorn, J. aan de Stegge, and W. Hoving, Phys. Rev. Lett. **68**, 2688 (1992).
[6] A. Fuss, S. Demokritov, P. Grünberg, and W. Zinn, J. Magn. Magn. Mater. **103**, L221 (1992).
[7] P.M. Levy, K. Ounadjela, S. Zhang, Y. Wang, C.B. Sommers, and A. Fert, J. Appl. Phys. **67**, 5914 (1990).
[8] F. Herman, J. Sticht, and M. van Schilfgaarde, J. Appl. Phys. **69**, 4783 (1991).
[9] F. Herman, J. Sticht, and M. van Schilfgaarde, in *Magnetic Thin Films, Multilayers and Surfaces* (Ref. 3), p. 195.
[10] H. Hasegawa, Phys. Rev. B **42**, 2368 (1990).
[11] D. Stoeffler and F. Gautier, Prog. Theor. Phys. Suppl. **101**, 139 (1990).
[12] D. Stoeffler, K. Ounadjela, and F. Gautier, J. Magn. Magn. Mater. **93**, 386 (1991).
[13] Y. Yafet, Phys. Rev. B **36**, 3948 (1987).
[14] W. Baltensberger and J.S. Helman, Appl. Phys. Lett. **57**, 2954 (1990).
[15] C. Chappert and J.P. Renard, Europhys. Lett. **15**, 553 (1991).
[16] D.M. Deaven, D.S. Rokhsar, and M. Johnson, Phys. Rev. B **44**, 5977 (1991).
[17] R. Coehoorn, Phys. Rev. B **44**, 9331 (1991).
[18] P. Bruno and C. Chappert, Phys. Rev. Lett. **67**, 1602 (1991); **67**, 2592(E) (1991).
[19] J. Friedel, Nuovo Cimento Suppl. **7**, 287 (1958).
[20] P.W. Anderson, Phys. Rev. **124**, 41 (1961).
[21] T. Moriya, *Spin Fluctuations in Itinerant Electron Magnetism* (Springer-Verlag, Berlin, 1985), Chap. 6.
[22] Y. Wang, P.M. Levy, and J.L. Fry, Phys. Rev. Lett. **65**, 2732 (1990).
[23] C. Lacroix and J.P. Gavigan, J. Magn. Magn. Mater. **93**, 413 (1991).
[24] P. Bruno (unpublished).
[25] M.A. Ruderman and C. Kittel, Phys. Rev. **96**, 99 (1954).
[26] T. Kasuya, Prog. Theor. Phys. **16**, 45 (1956).
[27] K. Yosida, Phys. Rev. **106**, 893 (1957).
[28] J.R. Schrieffer and P.A. Wolff, Phys. Rev. **149**, 491 (1966).
[29] L.M. Roth, H.J. Zeiger, and T.A. Kaplan, Phys. Rev. **149**, 519 (1966).
[30] Y. Yafet, J. Appl. Phys. **61**, 4058 (1987).
[31] Note that, in Ref. 18, a different convention was used: q_z^{α}

was taken positive, so that for negative q_z^α, the phases given there differ by π with those of the present paper.
[32] R.J. Celotta (private communication).
[33] F.C. Frank and J.H. van der Merwe, Proc. R. Soc. London, Ser. A **64**, 205 (1949); **64**, 216 (1949).
[34] E. Fawcett, R. Griessen, W. Joss, M.J.G. Lee, and J.M. Perez, in *Electrons at the Fermi Surface*, edited by M. Springford (Cambridge University Press, Cambridge, England, 1980), Chap. 7.
[35] M.R. Halse, Philos. Trans. R. Soc. London, Ser. A **265**, 507 (1969).
[36] D.H. Mosca, F. Petroff, A. Fert, P.A. Schroeder, W.P. Pratt Jr., R. Laloe, and S. Lequien, J. Magn. Magn. Mater. **94**, L1 (1991).
[37] S.S.P. Parkin, R. Bhadra, and K.P. Roche, Phys. Rev. Lett. **66**, 2152 (1991).
[38] F. Petroff, A. Barthélemy, D.H. Mosca, D.K. Lottis, A. Fert, P.A. Schroeder, W.P. Pratt, Jr., R. Laloe, and S. Lequien, Phys. Rev. B **44**, 5355 (1991).
[39] J.J. de Miguel, A. Cebollada, J.M. Gallego, R. Miranda, C.M. Schneider, P. Schuster, and J. Kirschner, J. Magn. Magn. Mater. **93**, 1 (1991).
[40] W.R. Bennett, W. Schwarzacher, and W.F. Egelhoff, Jr., Phys. Rev. Lett. **65**, 3169 (1990).

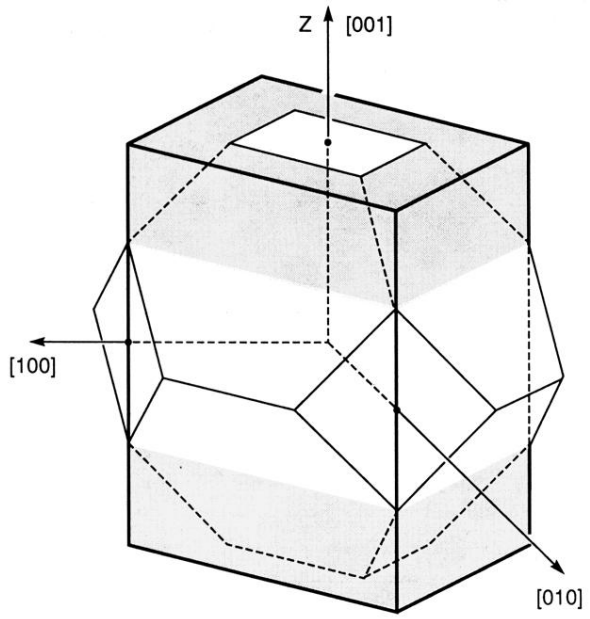

FIG. 3. First Brillouin zone of the fcc lattice (thin lines), and auxiliary zone for the (001) orientation (bold lines).

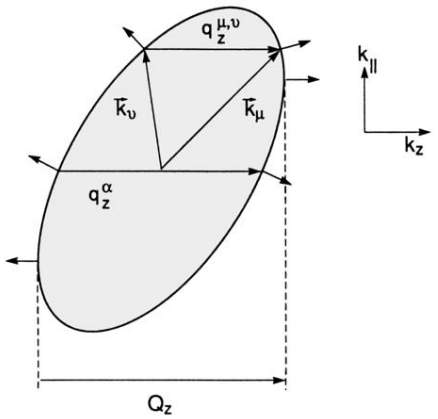

FIG. 4. Sketch showing the wave vector $q_z^{\mu,\nu}$ and the stationary vector q_z^{α}. The calliper Q_z of Roth, Zeiger, and Kaplan (Ref. 29) is also shown. The small arrows are the velocity vectors. See text for further explanations.

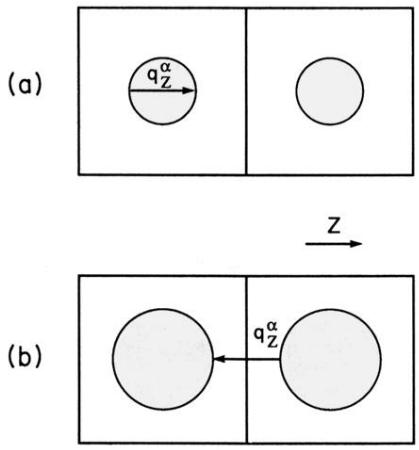

FIG. 5. Sketch explaining the sign convention for q_z^α. (a) q_z^α is "inside" the Fermi surface, i.e., positive; (b) q_z^α is "outside" the Fermi surface, i.e., negative.